

Effect of Overdispersion of Lethal Lesions on Cell Survival Curves

M. Loan^{a*} and A. Bhat^b

^a*ANUC, Australian National University, Canberra, 2600, Australia*

^b*Department of Oncology, East Tennessee State University, Tennessee, 37614, USA*

(Dated: February 17, 2022)

Purpose: The linear-quadratic (LQ) model is one of the most commonly used tools for predicting radiotherapy outcomes and has been used extensively to analyse dose responses to ionizing radiation both in vitro and in vivo. However, there remain questions about the wider applicability of the LQ model in terms of its representative nature of some deeper mechanistic behaviour. In particular, empirical evidence suggests that the LQ model tends to underestimate cell survival at low doses and overestimate cell killing at high doses. It is believed to be driven from the usual LQ model assumption that radiogenic lesions are Poisson distributed. In this context, we explore the effects of over dispersed DNA lesion distribution on the shapes of cell surviving curves of mammalian cells exposed to hadrons at various doses.

Methods: To provide a theoretical framework in resolving discrepancies between experimental data and LQ model predictions, we employ a non-Poisson distribution of lethal lesions together with non-homologous end-joining (NHEJ) pathway of double-strand break (DSB) repair. A negative binomial (NB) distribution is used to study the effect of the overdispersion on the shapes and possible reduction of dose-response curvature at high doses. The error distribution is customized to include an adjustable parameter so that the overdispersion parameter of NB is not constant but depends on the mean of the distribution. The trends in predicted cell survival responses are compared with the experimental data in low and high dose regions at various LET values for proton, helium, and carbon ions.

Results and Conclusions: The cell survival responses calculated by the present method reveal straightening of survival curves at high doses. This suggests that the overdispersion causes the cell survival dose-response to approximate log-linear behaviour at high doses. Comparison of the cell survival predictions with the Particle Irradiation Data Ensemble (PIDE) shows that the NB model provides better fits to the experimental data following low and intermediate doses. Whereas the model predictions are not validated at tiny and very high doses, nonetheless, the presented approach provides insight into underlying microscopic mechanisms which may help to improve the radiobiological responses along the dose-response curves and resolve discrepancies between experimental data and current cell survival models.

Keywords: Linear-quadratic model, non-Poisson distribution, dose-response, hadron therapy

arXiv:2110.05795v1 [physics.med-ph] 12 Oct 2021

* Corresponding author

I. INTRODUCTION

It has long been established that the linear-quadratic (LQ) model is a preferred mechanism for quantitative predictions of the description of radiation-induced cell death and chromosomal aberration dose responses using sufficiently few adjustable parameters. Underlying the application of the LQ model to fractionation effects is pairwise misrepair of primary lesions, which are resolved either through restitution or binary misrepair. It is assumed that the frequency of chromosomal aberrations is a linear-quadratic function of dose because the aberrations are consequences of the interaction of two separate DNA breaks. At low doses per fraction, both breaks may be caused by the same ionization event; the probability of exchange aberration is proportional to the dose. At the higher doses, the two breaks are more likely to be caused by multiple hits, the probability of exchange aberration is proportional to the square of the dose. The model has also proved to be a good approximation to a wide range of damage-kinetic models which describe the kinetics of DNA double-strand breaks [1–7]. Whereas these models have different formulations for the dose dependence of the mean lethal lesion yield, the common feature of explaining clonogenic cell survival is the Poisson distribution of the mean number of lethal lesions per cell. Such assumptions are understandable, given that these models evolved to explain clonogenic cell survival, an endpoint for which the number of lesions in individual cells cannot be quantified. Overall, these mechanisms produce a linear-quadratic-linear dose-response relationship at low LET [8–16].

However, despite the widespread usage of the LQ model, there remain questions about its wider applicability [17, 19–21]. For example, there is growing evidence that indicates that the LQ model exhibits a departure from of its linear quadratic relation at very low and very high doses. It has been observed that in the phenomenon of low-dose hypersensitivity, some cells show dramatic sensitivity to low doses < 0.5 Gy, before returning to an LQ-like response at higher doses [22]. Studies have shown that the dose-response curve begins to straighten at higher doses, leading some investigators to propose that a linear-quadratic-linear dose-response model is more appropriate [23]. The discrepancy between the measured cell survival data and the LQ model predictions at a higher dose is explained by the heterogeneity of sensitivity to radiation among the cells of the irradiated population [24–27]. Postulating that increasing LET causes non-random clustering of lethal lesions in some cells to deviate from the Poisson distribution, Hawkins reported a detailed study on the effect of deviation from the Poisson distribution of lethal lesions on the dependence of RBE in the limit of zero dose on the LET greater than that of linear range [28–30]. Using a Compound Poisson distribution, Nowak *et al.*, modelled the clustering of breakage events as the process leading to non-exponential “spacing” between subsequent events, to relate parameters of such distributions to relevant quantities describing the number of induced DSBs [31–33]. More recently, Shuryak [34, 35] reported the evidence of overdispersion by comparing the fits to the fibroblasts data from a Poisson distribution and the Negative Binomial distribution. The study reported that the Poisson distribution underestimated the “upper tail” of the observed distribution.

Using a non-Poisson approach as a more flexible alternative that allows accommodating a variety of mechanisms for overdispersion, we employ a customized negative binomial (NB) distribution to calculate the survival probabilities of V79 cell lines radiated by hadrons and light ions. For higher LET radiations, the individual particle tracks can infer multiple instances of lethal damage, and the ratio of the variance of the distribution to the mean of the distribution exceeds unity. The use of such a non-Poisson distribution implicitly determines the density and spatial distribution of DSB within and among cells. That is, DSB formed along high LET particle tracks tends to be in closer spatial proximity than DSB formed by different particle tracks. The rest of the paper is organised as follows: In Sec.II, we develop an NB error model for cell survival fraction in terms of modified radiosensitive parameters. The DSB repair kinetics is described using the non-homologous end-joining pathway. Biologically relevant quantities, such as radiosensitive parameters, are further derived and used to obtain the fit parameters of the model. The model is tested against PIDE and other observed data in Sec.III. The results of these comparisons provide useful information on how changing the error distribution for radiation-induced lethal lesions from Poisson to NB, without changing the LQ dose dependence for the mean, alters the performance of the LQ model in describing survival curve predictions at high doses and low doses/dose rates.

II. MODEL CALCULATION OF SURVIVAL FRACTION

A. Radiation Induced Average DSB Yield

Following the LQ model, the mean number of lethal lesions per cell, λ , is described by

$$\lambda = -\alpha D - \beta D^2, \quad (1)$$

where α and β are the model parameters describing the radiosensitivity of cell and D is the radiation dose. Assuming the lethal lesions are Poisson distributed from cell to cell, the probability of k lethal lesions in a cell is given by

$$P_{Pois.}(k) = \frac{\lambda^k e^{-\lambda}}{k!}. \quad (2)$$

and cell surviving probability is given by

$$SF_{Pois.} = P_{Pois.}(k=0) = e^{-\lambda}. \quad (3)$$

It has been well established that the effective plot of Eq. (3), on a log scale, gives what is referred to as a "shouldered" dose-response curve. The initial region of the curve is dominated by the linear term at low doses, followed by increasing curvature as the quadratic term becomes more significant. The degree of curvature is commonly expressed in terms of the α/β ratio and corresponds to the dose at which the linear and quadratic contributions are equal. To incorporate the effects of the overdispersed lethal chromosomal lesions among cells, we employ a customized negative binomial (NB) distribution. The probability of observing k lethal lesions in a cell in such an error distribution is described by

$$P_{NB}(k) = \frac{\Gamma(k+1/\omega)}{\Gamma(1/\omega) \times k!} \left(\frac{1}{1+\omega\lambda} \right)^{1/\omega} \times \left(\frac{1}{1+1/\omega\lambda} \right)^k. \quad (4)$$

where $\omega = r(1 - e^{-\lambda})$ is the modified dispersion parameter relative to the Poisson distribution and describes the dependence of bare dispersion parameter r on the mean λ that results from the possibility that at low λ overdispersion can be negligibly small but is expected to increase to a certain limit at higher values of λ . It is expected that small values of r (close to zero) generate Poisson distribution-like behaviours, whereas larger r values produce distributions with larger tails [34]. The NB error modelled surviving fraction becomes

$$SF_{NB} = P_{NB}(k=0) = (1 + \omega\lambda)^{-1/\omega}. \quad (5)$$

Following [36], we first calculate the average number of primary particles that cause DSB, n_p , and the average number of DSBs yielded by each primary particle that causes DSB, λ_p . The DSB yield per cell per primary particle is given by $\lambda = N/n$, where $N = YD$ is the average number of radiation induced DSBs per cell and n is the number of the particles passing through the cell nucleus

$$n = \frac{\pi R^2 D \rho}{0.160 \times LET}, \quad (6)$$

where R is the cell nucleus radius (μm) and ρ is density (g/cm^3). Assuming that the number of DSBs yielded by a primary particle is NB distributed, the probability of a primary particle passing through a nucleus without causing any DSB is given by

$$P_{NB}(k=0) = (1 + \omega\lambda)^{-1/\omega}. \quad (7)$$

The average number of primary particles that cause DSB, n_p , and the average number of DSBs yield per primary particle that causes DSB, λ_p , are then given by

$$n_p = n[1 - (1 + \omega\lambda)^{-1/\omega}], \quad (8)$$

$$\lambda_p = \frac{\lambda}{[1 - (1 + \omega\lambda)^{-1/\omega}]}. \quad (9)$$

B. Cell Survival Curve

Double strand breaks in DNA form as a result of exposure to exogenous agents such as radiation and certain chemicals, as well as through endogenous processes, including DNA replication and repair. Three DSB repair processes, the non-homologous end-joining (NHEJ) pathway, the homologous recombination repair (HRR) pathway, and the Mismatch End Joining (MMEJ) are commonly used in mammalian cells with NHEJ likely playing the largest role in DSB repair [37–39]. NHEJ mediates the direct rejoining of the broken DNA molecule [40] and has the potential to bind together any type of DNA ends and does not require a homologous template for repair of the DNA lesion. Unlike HRR, the non-homologous end-joining (NHEJ) pathway is not restricted to a certain phase of the cell cycle. Recent studies [41, 42] indicate that the relationship between radiation dose and the number of DNA fragments shorter than 30 bp induced by radiation is considered to be linear. This indicates that, other than the interaction among DSBs induced by different primary particles, both the clustered DNA damage effect (two or more DSBs within a typical distance of 25 bp) and the overkill effect (two or more DSBs within 10 bp) of high LET radiation depend mainly on the DSB distribution on the track of the primary particles. Therefore, both effects depend on the average number of DSBs yield by each primary particle that caused DSB, λ_p . The average number of lethal events, N_p , can be modelled by

$$N_{avg} = N \times (1 - P_{correct}), \quad (10)$$

where $P_{correct}$ is the total probability of a DSB being correctly rejoined. For any break in a particular condition, the true distribution of rejoining rates is non-trivial and lacks a simple form for its overall distribution. Following [43], the repair behaviour is determined by approximating the recombination function to a step function where the break in question will have the same recombination rate for all potential breaks occurring at distance d_{max} within a shell of radius R. This simplifies the probability of correct repair for a given break to $1/(1+k)$, where k is the number of breaks within the distance d_{max} [43].

Following the general mechanism of NHEJ, each DSB may be (i) rejoined with the other end from the same DSB, (ii) joined with a DSB end from a different DSB induced by the same primary particle, (iii) joined with a DSB end from a DSB induced by a different primary particle, and (iv) left without being joined with any DSB end. Each pathway has an associated fidelity which indicates the probability with which the pathway will correctly repair a given DSB. The average probability that the DSB is correctly joined with the other end from the same DSB is assumed to be μ_x , which quantitatively describes the fidelity of the NHEJ pathway [36, 38].

Assuming that the breaks within the spherical radius are NB distributed, the expectation value that a randomly chosen break will rejoin correctly (a DSB end do not be joined with a DSB end from a DSB induced by a different primary particle) is given by (see the Appendix)

$$P_1 = \frac{1}{\lambda_{int}(1-\omega)} \left[1 - (1 + \omega\lambda_{int})^{1-1/\omega} \right], \quad (11)$$

where $\lambda_{int} = \eta(\lambda_p)n_p$ is the average probability of a DSB end being joined with a DSB end from a DSB induced by a different primary particle and is proportional to the average number of primary particles which caused DSBs, n_p . The relationship between $\eta(\lambda_p)$ and λ_p is assumed as [36]:

$$\begin{cases} \eta(\lambda_p) &= \eta_{\lambda_p \rightarrow \infty} - \frac{\eta_{\lambda_p \rightarrow \infty} - \eta_{\lambda_p \rightarrow 1}}{\lambda_p} \\ \lim_{\eta_{\lambda_p \rightarrow 1}} \eta(\lambda_p) &= \eta_{\lambda_p \rightarrow 1} \\ \lim_{\eta_{\lambda_p \rightarrow \infty}} \eta(\lambda_p) &= \eta_{\lambda_p \rightarrow \infty}. \end{cases}$$

Also, assuming that a primary particle generates DSBs randomly on its track, the probability that a DSB end not be joined with a DSB end from a different DSB induced by the same primary particle is given by

$$P_2 = \frac{1}{\lambda_{track}(1-\omega)} \left[1 - (1 + \omega\lambda_{track})^{1-1/\omega} \right], \quad (12)$$

where $\lambda_{track} = \phi\lambda_p$ is the average probability of a DSB end being joined with a DSB end from a DSB induced by the same primary particle. Therefore, the total probability of a DSB being correctly repaired is given by

$$\begin{aligned} P_{correct} &= \mu_x P_1 P_2 \\ &= \mu_x \left[\frac{1}{\lambda_{int}(1-\omega)} \left(1 - (1 + \omega\lambda_{int})^{1-1/\omega} \right) \right] \times \left[\frac{1}{\lambda_{track}(1-\omega)} \left(1 - (1 + \omega\lambda_{track})^{1-1/\omega} \right) \right]. \end{aligned} \quad (13)$$

The first term in the square brackets quantitatively describes the interaction of DSBs induced by different primary particles and the second term describes the effect of clustered DNA damage.

Finally, considering the overkill effect, similar with the clustered DNA damage effect from Eq.(12), the probability of a DSB having contributed to cell death is given by:

$$P_3 = \frac{1}{\lambda_{contb.}(1-\omega)} \left[1 - (1 + \omega\mu_{contb.})^{1-1/\omega} \right], \quad (14)$$

where $\lambda_{contb.} = \xi\lambda_p$.

Using the above repairing probabilities, Eq. (10) becomes

$$N_{avg} = \frac{N}{\lambda_{contb.}(1-\omega)} \left[1 - (1 + \omega\lambda_{contb.})^{1-1/\omega} \right] \times \left[1 - \lambda_x \left\{ \frac{1}{\lambda_{int}(1-\omega)} \left(1 - (1 + \omega\lambda_{int})^{1-1/\omega} \right) \right\} \right. \\ \left. \times \left\{ \frac{1}{\lambda_{track}(1-\omega)} \left(1 - (1 + \omega\lambda_{track})^{1-1/\omega} \right) \right\} \right], \quad (15)$$

and the cell survival takes the form:

$$S_{NB} = \left(1 + \omega N_{avg} \right)^{-1/\omega} = \left(1 + \omega(\alpha_{NB}D + \beta_{NB}D^2) \right)^{-1/\omega}, \quad (16)$$

where

$$\alpha_{NB} = \frac{Y}{\xi\lambda_p(1-\omega)} \left(1 - (1 + \omega\xi\lambda_p)^{1-1/\omega} \right) \left[1 - \mu_x \frac{1}{\phi\lambda_p(1-\omega)} \left(1 - (1 + \omega\phi\lambda_p)^{1-1/\omega} \right) \right] \quad (17)$$

$$\beta_{NB} = \frac{1}{2} \frac{\eta(\lambda_p)}{\lambda_p} \frac{\mu_x Y^2}{\xi\lambda_p(1-\omega)} \left(1 - (1 + \omega\xi\lambda_p)^{1-1/\omega} \right) \frac{1}{\phi\lambda_p(1-\omega)} \left(1 - (1 + \omega\phi\lambda_p)^{1-1/\omega} \right) \quad (18)$$

are the modified radiosensitive parameters of the model.

C. Model Fitting Parameters

To obtain the over-dispersion parameter that maximizes the likelihood of making the observations given the parameters, we fit the NB distribution (Eq. (5) with $\omega = r$) to the survival data on 1.15 MeV proton irradiated V79 cells and 25 MeV helium ion irradiated T1 cells [44]. A log-likelihood maximization was performed across the analysed cells to find the best-fit value for a particular data set. The NB log-likelihood function was performed using the parmhat function that specifies control parameters for the iterative algorithm the function uses. The programming was implemented in MATLAB ©R2019a software. At 95% confidence intervals, the value of r was found to be 0.043 and 0.241, for the lower and upper limits, respectively. The bare overdispersion parameter was set to a constant value of 0.142, the best-fit value for data on V79 cell survival.

The yield of DSBs induced by hadrons and light ions was directly calculated with fast Monte Carlo damage simulation (MCDS) software [45]. This algorithm captures the trend in the DNA damage spectrum with the possibility that the small-scale spatial distribution of elementary damages is governed by stochastic events and processes [46, 47]. It has been observed that the MCDS algorithm gives reliable results of the damage yields that are comparable to those obtained from computationally expensive but more detailed track structure simulations. For MCDS simulations, the results of DNA damage yields for protons and light ions are usually obtained within minutes. The random Gaussian error is added by repeating the simulation 10 times for each LET value to generate ten ensembles of DSB yield measurements for each LET value for later analysis. The expectation values and statistical errors were estimated using the jackknife method. With Y and λ obtained with MCDS, and ω obtained as above, n_p and λ_p were obtained by using Eqs. (8) and (9).

Fig.1 shows the average number of DSBs yielded by each primary particle that cause DSB, λ_p , as a function of LET. For a constant dose, DSB yield per track changes more quickly with LET. This is as expected since the number of primary particles passing through the cell nucleus is inversely proportional to LET. The results show that for protons at $LET \leq 10$ keV/ μ m, λ_p increases rather slowly and has similar behaviour to that of photons in this LET region. This may be one of the reasons why the relative biological effectiveness of low LET protons is similar to that of photons. With protons, a two-fold increase in λ_p is observed when LET was increased from 10 to 60 keV/ μ m. whereas λ_p

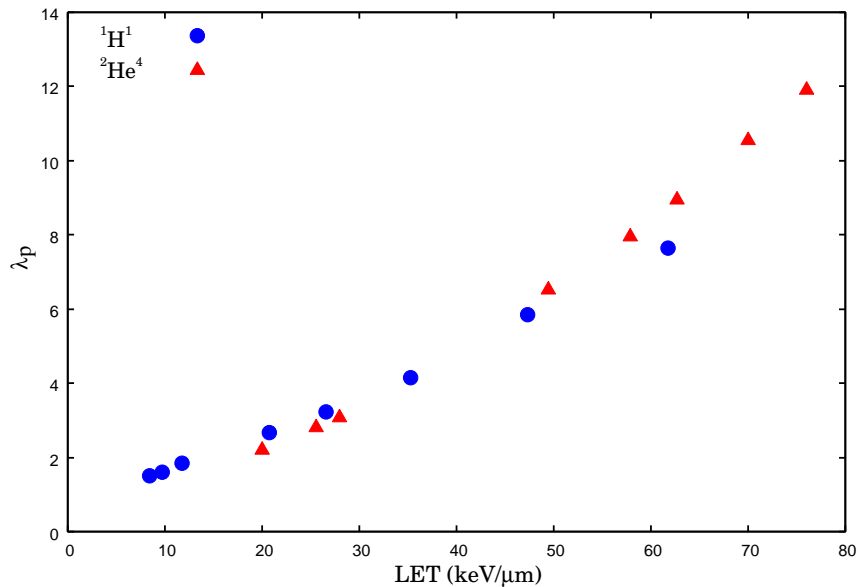


FIG. 1: DSBs yielded by each primary particle that cause DSB, λ_p , of V79 cells irradiated with protons and helium ions.

increases relatively quickly with helium ions at high LET, the difference between λ_p values for protons and helium ions is negligible for $20 < \text{LET} < 30 \text{ keV}/\mu\text{m}$. This is expected since ion LET is understood to modulate radiosensitivity through different patterns of energy deposition: higher LET radiations are more densely ionizing, which results in an increased DNA-double strand break (DSB) yield and clustered DSB yield per unit dose [42]. Also, for the same LET, different ions will have differing DNA damage yields due to differing track ionization densities, e.g., a He-ion will have a higher DSB and clustered DSB yield compared to a C-ion of the same LET due to its much denser track [42].

TABLE I: Best fit parameters of the model for V79 cell

Parameters	NB model	NB(χ^2/N_{df})	Poisson model	Pois(χ^2/N_{df})
Cell radius	$5.4 \pm 0.2 \mu\text{m}$			
Overdispersion r	0.146			
μ_x	0.9561 ± 0.0235	0.872	0.9794 ± 0.0163	0.931
ϕ	0.0608 ± 0.0381		0.0593 ± 0.0212	
ξ	0.0398 ± 0.0129		0.0412 ± 0.0209	
$\eta\lambda_p \rightarrow 1$	$(9.386 \pm 0.104) \times 10^{-4}$	0.764	$(9.785 \pm 0.120) \times 10^{-4}$	0.886
$\eta\lambda_p \rightarrow \infty$	0.0065 ± 0.0001	0.812	0.0068 ± 0.0001	0.823

The parameters μ_x , ϕ , and ξ were obtained by fitting the experimental data of cell survival curves of V79 cells [48]. Twenty data sets for cell survival were selected to cover a wide range of high, medium, and low surviving fractions, allowing a detailed analysis of survival curve shapes. GRABIT Data Figure Digitizer routine in MATLAB was used to estimate data points and error bars from published graphs. First, the parameters μ_x , ϕ and ξ were obtained by fitting the experimental data of α values and the calculated n_p and λ_p values with Eq.(17). Using these values together with the experimental data of cell survival for V79 cells exposed in X-rays, we obtained $\eta\lambda_{p \rightarrow 1}$ with Eq.(16). Finally, $\eta\lambda_{p \rightarrow \infty}$ was obtained by fitting the experimental data with Eq.(18). The goodness of the fits was gauged by the reduced chi-squared test using the GNU plot. The best fit values and their uncertainties are summarised in Table I.

III. RESULTS AND DISCUSSION

Using the parameters obtained above, we evaluate and display the effect of overdispersed lesions for V79 cells, irradiated by protons at low and high doses for different LET values, in Fig.2. Comparing the NB and Poisson model dose-response predictions, (Fig.2 a-c), to the data in the Particle Irradiation Data Ensemble (PIDE) [49], we observe that the Poisson model agrees well with the experimental data at doses ≤ 2 Gy but underestimates the “lower tail” of the observed distribution at medium and higher doses. On the other hand, NB error distribution outperforms the Poisson model and shows a good agreement with the experimental values at medium and higher doses for all LET values explored here. A closeup of the dose-response curve for improved visualization of the modelled fits (Fig.2-d)

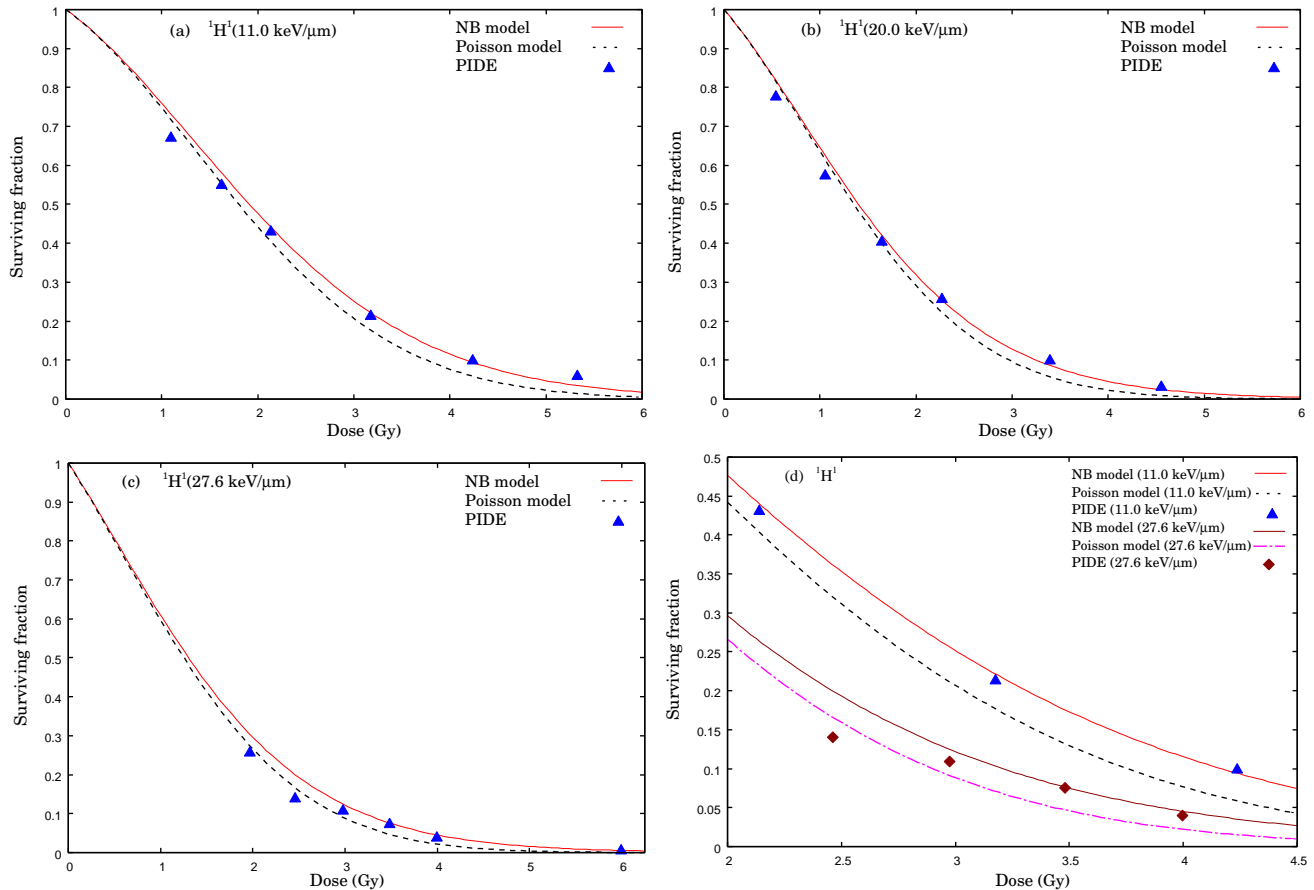


FIG. 2: Comparison between measured (PIDE [49] - solid symbols) and model cell survival fractions (solid and dashed lines) for V79 cells irradiated by protons at different LET. Magnified dose-response curves for improved visualization of the modelled fits are shown in panel d.

shows straightening of dose-response in the intermediate dose region. This indicates that overdispersion causes the dose-response curves to approximate log-linear behaviour at high doses. This is because overdispersion alters the relationship between the mean number of lethal lesions per cell and survival (the probability of a cell having zero lethal lesions). It is obvious that with the same mean number of lethal lesions per cell, NB distribution predicts a larger probability of a cell to contain zero lethal lesions than that predicted by the Poisson distribution. This effect is expected to increase with the increasing mean number of lethal lesions per cell and with increasing overdispersion as the damage saturation correction implies that a further increase in damage within tracks does not further increase cell killing. The important consequence is that at radiation doses that kill most cells by producing a large mean number of lethal lesions per cell, the Poisson distribution can predict substantially lower cell survival probabilities than the overdispersed NB distribution.

For the same cell type, the NB error model showed enough flexibility to describe the surviving fraction not only for the particle types used in model parameter fitting but also for different types of particles at different LET. Fig.3

shows the evidence for overdispersion of lethal lesions was also found at relevant doses for V79 cells irradiated by helium and carbon ions at different LET. The effective plots (Fig.3 - a and b) show that the NB error distribution

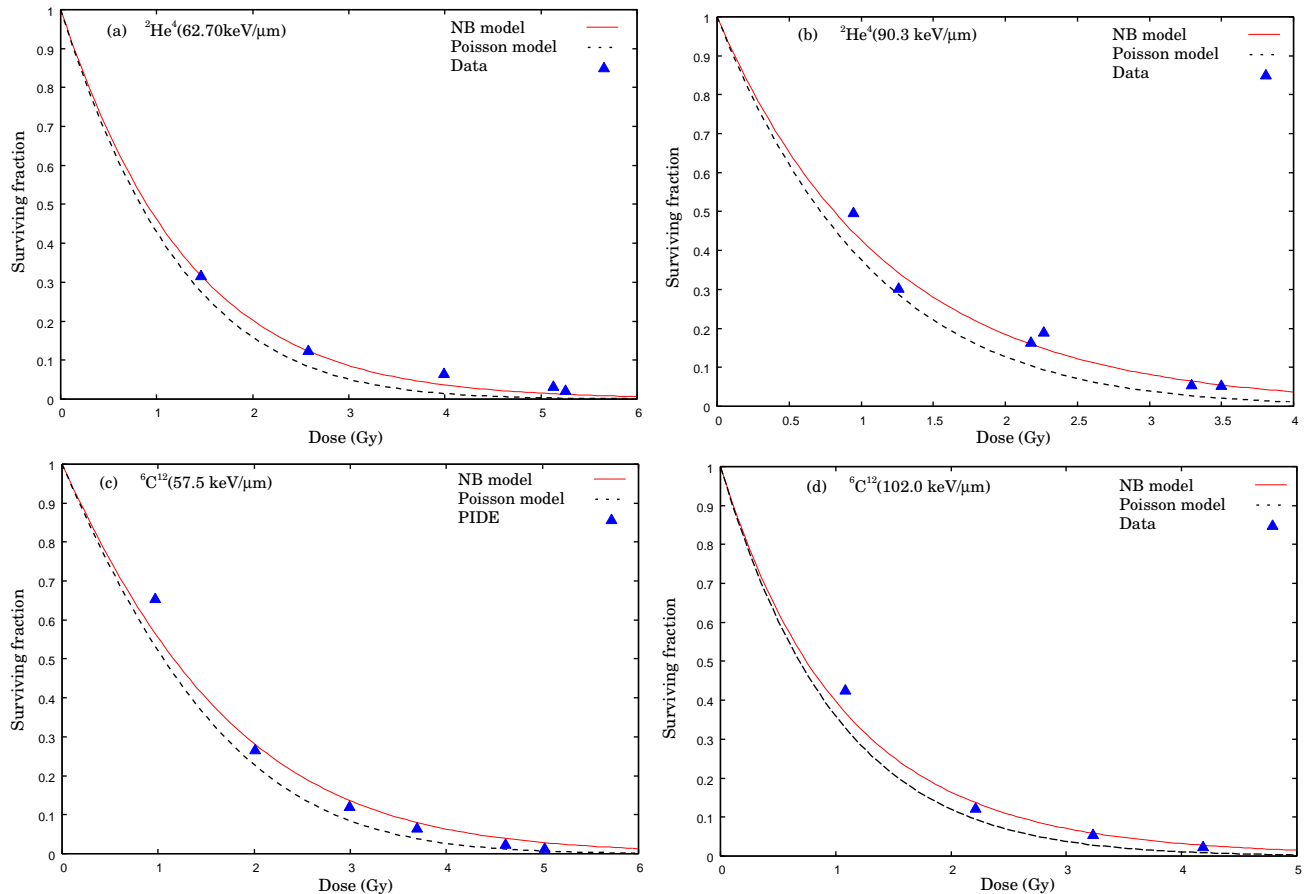


FIG. 3: Comparison between experimental data (PIDE [49], Data [50]) of cell surviving fractions (points) and modelled results (solid and dashed lines) for V79 cells irradiated by helium and carbon ions.

predictions with helium ions are considerably closer to the measured cell survival data [49, 50] at doses > 2 Gy. To quantify the agreement between the predicted and measured survival fractions, we evaluated the Poisson and NB error modelled cell survival probabilities at various doses. In contrast to NB distribution, the Poisson modelled survival curves predict 27.8, 8.5, 1.37, and 0.3% survival fractions at 1.47, 2.58, 4.0, and 5.25 Gy relative to 31.9, 12.4, 6.2, and 2.06% measured fractions, respectively. The corresponding zero lethal lesion probabilities predicted by the NB error model are 31.9, 12.4, 3.67, and 1.37% are considerably closer to the measured data. The comparison reveals that the Poisson model tends to produce fits away from the measured values at higher doses of helium ions. These results provide support for our contention that the distribution of lethal chromosomal lesions per cell at high doses of ionizing radiation may not be optimally described by the Poisson distribution. Alternative approaches such as the NB distribution, which allows the variance to be larger than the mean, allow better fits to such data. The added flexibility can translate into better descriptions of available survival dose-response data, and better predictions of the dose responses at low doses/ dose rates, as well as at high doses. For example, moderate overdispersion of lethal lesions per cell modelled by the NB distribution substantially modifies BED estimates for radiotherapy regimens that use three to five dose fractions of ≥ 5 Gy/fraction.

Our analysis of dose-response with carbon ions at 57.7 and 102 keV/ μm shows that Poisson modelled cell survival trends moderately underestimate the actual survival data at medium doses. This is in contrast to the cell survival probabilities with proton and helium ions, the Poisson distribution describes the measured data for the doses ≥ 4.65 Gy. This might be due to the reason that the ionization density of carbon ions induces more complex DNA damage which makes the DNA repair process complex, partially due to retarded enzymatic activities, leading to increased chromosome aberrations and cell death. This suggests that, in general, the repair process following heavy-ion exposure

is LET-dependent, but with nonhomologous end-joining defective cells, this trend is less emphasized.

IV. CONCLUSIONS

We adopted the effect of a customized negative binomial distribution as a more flexible approach that accounts for the non-random clustering and overdispersion of lethal lesions and evaluated the modifications in shapes of cell survival response curves. The NB error distribution response model was tested by fitting the cell survival predictions to the measured data for V79 cells irradiated with LETs within the range of 11– 102 keV/ μm . The model provides good agreement with experimental cell survival data in the medium and high dose regions for the range of LET investigated, confirming the effectiveness of the parameterization method. These results from lymphocytes and fibroblasts provide support for our contention that the distribution of lethal chromosomal lesions per cell at high doses of radiation may not be optimally described by the Poisson distribution. Alternative approaches, such as the NB distribution, which allows the variance to be larger than the mean, allow for better fitting of such data. Although there are other explanations for cell survival curve straightening at high doses, our results do not contradict these explanations, since a non-Poisson error distribution of lethal lesions and a non-LQ dose dependency are not mutually exclusive. Therefore, we do not choose to advocate one over the other. We argue, however, that even with a continuously curving dose-response formalism and an overdispersed error distribution straightening of survival curves at high doses can be explained without causing other fundamental questions about the relationship between dose and average number of lethal events. Taking the error distribution into consideration may be a useful approach for modelling the effects of modern radiotherapy with high doses per fraction. Such adjustments within an improved NB distribution can potentially improve radiobiological modelling at high-dose cancer radiotherapy and may be useful for optimization of radiotherapy treatment planning to maximize tumour control.

Conflict of Interest

No conflict of interest to declare.

-
- [1] H. Thames, *An incomplete-repair model for survival after fractionated and continuous irradiations*, Int. J. Radiat. Biol., **47**, 319 (1985)
 - [2] R. Preston, *Mechanisms of induction of specific chromosomal alterations*, Basic Life Sci., **53**, 329 (1990)
 - [3] L. Gerweck, S. Zaidi, A. Zietman, *Multivariate determinants of radiocurability I: Prediction of single fraction tumor control doses*, Int. J. Radiat. Oncol. Biol. Phys., **29**, 57 (1994)
 - [4] R. Sachs, P. Hahnfeld and D. Brenner, *The link between low-LET dose-response relations and the underlying kinetics of damage production/repair/misrepair*, Int. J. Radiat. Biol., **72**, 351 (1997)
 - [5] R. Stewart, *Two-Lesion Kinetic Model of Double-Strand Break Rejoining and Cell Killing*, Radiat. Res., **56**, 365 (2001)
 - [6] M. Guerrero, R. Stewart, J. Wang and X. Li, *Equivalence of the linear-quadratic and two-lesion kinetic models*, Phys. Med. Biol., **47**, 3197 (2002)
 - [7] M. Brown, R. Bristow, P. Glazer, R. Hill, W. McBride, G. McKenna and R. Muschel, *Comment on Tumor response to radiotherapy regulated by endothelial cell apoptosis (II)*, Science, **302**, 1894 (2003)
 - [8] S. Curtis, *Lethal and potentially lethal lesions induced by radiation - a unified repair model*, Radiat. Res., **106**, 252 (1986)
 - [9] H. Rossi and M. Zaider, *Saturation in dual radiation action*, Proceedings of the Symposium on Quantitative Mathematical Models in Radiation Biology, 111 (1988), Springer, Berlin
 - [10] D. Brenner, *Track structure, lesion development, and cell survival*, Radiat. Res., **124**, S29 (1990)
 - [11] G. Obaturov, V. Moiseenko and A. Filimonov, *Model of mammalian cell reproductive death. I. Basic assumptions and general equations*, Radiat. Environ. Biophys., **32**, 285 (1993)
 - [12] C. Tobias, *The repair-misrepair model in radiobiology: comparison to other models*, Radiat. Res. Suppl., **8**, S77 (1985)
 - [13] R. Hawkins, *A microdosimetric-kinetic model of cell death from exposure to ionizing radiation of any LET, with experimental and clinical applications*, Int. J. Radiat. Biol., **69**, 739 (1996)
 - [14] T. Radivoyevitch, D. Hoel, A. Chen and R. Sachs, *Misrejoining of double-strand breaks after X irradiation: Relating moderate to very high doses by a Markov model*, Radiat. Res., **149**, 59 (1998)
 - [15] D. Brenner, L. Hlatky, P. Hahnfeldt, Y. Huang and R. Sachs, *The linear-quadratic model and most other common radiobiological models result in similar predictions of time-dose relationships*, Radiat. Res., **150**, 83 (1998)
 - [16] M. Carlone, D. Wilkins and P. Raaphorst, *The modified linear-quadratic model of Guerrero and Li can be derived from a mechanistic basis and exhibits linear-quadratic-linear behaviour*, Phys. Med. Biol., **50**, L9 (2005)
 - [17] R. Sachs and D. Brenner, *The mechanistic basis of the linear-quadratic formalism* Med. Phys., **25**, 2071 (1998)

- [18] R. Hawkins, *A microdosimetric-kinetic theory of the dependence of the RBE for cell death on LET*, Med. Phys., **25**, 1157 (1998)
- [19] M. Zaider, *There is no mechanistic basis for the use of the linear-quadratic expression in cellular survival analysis*, Med. Phys., **25**, 791 (1998)
- [20] J. Kirkpatrick and D. Brenner and C. Orton, *The linear-quadratic model is inappropriate to model high dose per fraction effects in radiosurgery*, Med. Phys., **36**, 3381 (2009)
- [21] S. McMohan, *The linear quadratic model: usage, interpretation and challenges*, Phys. Med. Biol., **64**, 01TR01, (2019)
- [22] M. Joiner, B. Marples, P. Lambib, S. Short and I. Turesson, *Low-dose hypersensitivity: current status and possible mechanisms*, Int. J. Radiat. Oncol. Biol. Phys., **49**, 379 (2001)
- [23] M. Astrahan, *Some implications of linear-quadratic-linear radiation dose-response with regard to hypofractionation*, Med. Phys., **35**, 4161 (2008)
- [24] R. Hawkins, *Biophysical models, microdosimetry and the linear quadratic survival relation*, Ann. Radiat. Ther. Oncol., **1**, 1013 (2017)
- [25] J. Ward, *DNA damage produced by ionizing radiation in mammalian cells: Identities, mechanisms of formation, and reparability*, Prog Nucleic Acid Res. Mol. Biol., **35**, 95 (1988)
- [26] D. Goodhead, *Initial events in the cellular effects of ionizing radiations: Clustered damage in DNA*, Int. J. Radiat. Biol., **65**, 7 (1994)
- [27] J. Heilmann and G. Taucher-Scholz and G. Kraft, *Induction of DNA double-strand breaks in CHO-K1 cells by carbon ions*, Int. J. Radiat. Biol., **68**, 153 (1995)
- [28] R. Hawkins, *A Microdosimetric-Kinetic model for the effect of non-Poisson distribution of lethal lesions on the variation of RBE with LET*, Radiat. Res., **160**, 61 (2003)
- [29] R. Hawkins, *Effect of heterogeneous radiosensitivity on the survival, alpha beta ratio and biologic effective dose calculation of irradiated mammalian cell populations*, Clin. Transl. Radiat. Oncol., **4**, 32 (2017)
- [30] M. Loan, M. Alameen, A. Bhat and M. Tantary, *RBE with non-Poisson distribution of radiation induced strand breaks*, arXiv:2009.06802v2 [physics.med-ph] (2020)
- [31] E. Gudowska-Nowak, M. Kramer, G. Kraft and G. Taucher-Scholz, *Compound Poisson Statistics and Models of Clustering of Radiation Induced DNA Double Strand Breaks*, (2000), arXiv:physics/0011071v1 [physics.bio-ph]
- [32] R. Virsik and D. Harder, *Statistical interpretation of the overdispersed distribution of radiation-induced dicentric chromosome aberrations at high LET*, Radiat. Res., **85**, 13 (1981)
- [33] E. Goodwin, E. Blakely and C. Tobias, *Chromosomal damage and repair in G1-phase Chinese hamster ovary cells exposed to charged-particle beams*, Radiat. Res., **138**, 343 (1994)
- [34] I. Shuryak and B. Loucas and M. Cornforth, *Straightning beta: over-dispersion of lethal chromosome aberrations following radiotherapeutic doses leads to terminal linearity in the alpha-beta model*, Front Oncol., **7**, 318 (2017)
- [35] I. Shuryak and M. Cornforth, *Accounting for overdispersion of lethal lesions in the linear quadratic model improves performance at both high and low radiation doses*, Int. J. Radiat. Biol., **97**, 50 (2020)
- [36] W. Wang and C. Li and R. Qiu and Y. Chen and Z. Wu and H. Zhang and J. Li, *Modelling of cellular survival following radiation-induced DNA double-strand breaks*, Sci. Rep., **8**, 16202 (2018)
- [37] C. Karge and P. Peschke, *RBE and related modeling in carbon-ion therapy*, Phys. Med. Biol., **63**, 01TR02(35pp) (2017)
- [38] S. Burma, B. Chen and D. Chen, *Role of non-homologous end joining (NHEJ) in maintaining genomic integrity*, DNA Repair (Amst), **5**, 1042 (2006)
- [39] S. Malu, *et al.*, *Role of non-homologous end joining in V(D)J recombination*, Immunol Res., **54**, 233 (2012)
- [40] E. Weterings and D. Chen, *The endless tale of non-homologous end-joining*, Cell Res., **18**, 114 (2008)
- [41] G. Baiocco, *et al.*, *The origin of neutron biological effectiveness as a function of energy*, Sci. Rep., **6**, 34033 (2016)
- [42] W. Friedland, *et al.*, *Comprehensive track-structure based evaluation of DNA damage by light ions from radiotherapy-relevant energies down to stopping*, Sci. Rep., **7**, 45161 (2017)
- [43] S. McMahan, J. Schuemann, H. Paganetti and K. Prise, *Mechanistic modelling of DNA repair and cellular survival following radiation-induced DNA damage*, Sci. Rep., **6**, 33290 (2016)
- [44] K. Prise, M. Folkard, S. Davies and B. Michael, *The irradiation of V79 mammalian cells by protons with energies below 2 MeV. Part II. Measurement of oxygen enhancement ratios and DNA damage*, Int. J. Radiat. Biol., **58**, 261 (1990)
- [45] V. Semenenko and R. Stewart, *Fast Monte Carlo Simulation of DNA Damage Formed by Electrons and Light Ions* Phys, Phys. Med. Biol., **51**, 1693 (2006)
- [46] R. Stewart *et al.*, *Rapid MCNP simulation of DNA double strand break (DSB) relative biological effectiveness (RBE) for photons, neutrons, and light ions*, Phys. Med. Biol., **60**, 8249 (2015)
- [47] R. Stewart, *Induction of DNA damage by light ions relative to ^{60}Co gamma-rays*, Int. J. Part. Ther., **5**, 25 (2018)
- [48] Y. Furusawa, *et al.*, *Inactivation of aerobic and hypoxic cells from three different cell lines by accelerated ^3He -, ^{12}C - and ^{20}Ne -Ion beams*, Radiat. Res., **154**, 485 (2000)
- [49] T. Friedrich, U. Scholz, T. Elsassner, M. Durante and M. Scholz, *Systematic analysis of RBE and related quantities using a database of cell survival experiments with ion beam irradiation*, Int. J. Radiat. Biol., **54**, 494 (2013)
- [50] N. Tilly, A. Brahme, J. Carlsson and B. Clmelus, *Comparison of cell survival models for mixed LET radiation*, Int. J. Radiat. Biol., **75**, 233 (1999)

Appendix A

We use a customized negative binomial (NB) distribution for evaluating the probability of observing k lethal lesions in a cell

$$P_{NB}(k) = \frac{\Gamma(k + 1/\omega)}{\Gamma(1/\omega) \times k!} \left(\frac{1}{1 + \omega\lambda} \right)^{1/\omega} \times \left(\frac{1}{1 + 1/\omega\lambda} \right)^k.$$

The likelihood function for N iid observations (k_1, k_2, \dots, k_N) is given by

$$L_{NB} = \prod_{i=1}^N f(k_i)$$

from which the log-likelihood function can be written as:

$$l_{NB} = -\left(\frac{1}{\omega}\right) \times (1 + k + \omega) \times \ln(1 + \omega + \lambda) + k \times \left(\ln(\omega) + \ln(\lambda) \right) + \ln \left[\Gamma\left(\frac{1 + k + \omega}{\omega}\right) \right] - \ln[\Gamma(1 + k)] - \ln \left[\Gamma\left(\frac{1}{\omega}\right) \right].$$

Assuming that the correct repair distribution is NB distributed, the probability that a break will be repaired correctly is

$$\begin{aligned} P_{NB} &= \sum_{k=0}^{\infty} \frac{1}{1+k} P_{NB}(k) = \sum_{k=0}^{\infty} \frac{\Gamma(k + \omega)}{\Gamma(\omega)} \times \frac{1}{1+k} p^\omega (1-p)^k \\ &= \sum_{k=0}^{\infty} \frac{(k + \omega - 1)!}{(\omega - 1)! (k + 1)!} p^\omega (1-p)^k. \end{aligned}$$

If we let $k + 1 = s$ and $\omega - 1 = z$, then

$$\begin{aligned} P_{NB} &= \frac{p}{z(1-p)} \sum_{s=1}^{\infty} \frac{(s + z - 1)!}{s! (z - 1)!} p^z (1-p)^s \\ &= \frac{p\omega}{(1-\omega)(1-p)} (1 - p^{\frac{1}{\omega}-1}). \end{aligned} \tag{A1}$$

By fixing the average number of breaks equal to the expected interaction rate $\lambda (= \eta(\lambda_p)n_p)$, we can use this to calculate the total probability of misrepair as a function of λ_p . Using $p = 1/(1 + \omega\lambda)$, we expand Eq. (A1) to obtained

$$P_{NB} = \frac{1}{\lambda(1-\omega)} \left[1 - \left(1 + \omega\lambda \right)^{1-1/\omega} \right].$$